




























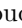









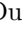
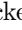
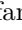
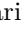

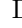

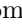

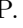

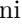
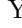





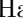

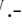
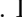


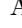

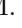
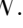

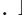
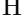


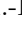
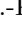
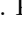
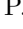
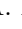

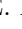
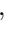
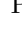
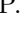

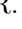
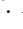
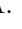
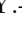
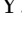


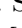
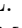
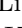


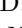



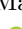
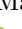
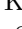
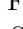
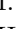
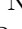
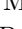




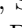

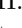
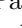
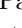


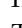







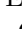










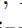



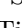
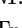










Search for Two-Body B Meson Decays to Λ^0 and $\Omega_c^{(*)0}$

V. Savinov , I. Adachi , J. K. Ahn , H. Aihara , D. M. Asner , H. Atmacan , R. Ayad , Sw. Banerjee , J. Bennett , M. Bessner , V. Bhardwaj , D. Biswas , A. Bobrov , D. Bodrov , J. Borah , M. Bračko , P. Branchini , T. E. Browder , A. Budano , D. Červenkov , M.-C. Chang , P. Chang , B. G. Cheon , K. Cho , S.-K. Choi , Y. Choi , S. Choudhury , N. Dash , G. De Nardo , G. De Pietro , R. Dhamija , F. Di Capua , J. Dingfelder , Z. Doležal , S. Dubey , P. Ecker , D. Epifanov , M. Farino , D. Ferlewicz , B. G. Fulsom , V. Gaur , A. Giri , P. Goldenzweig , E. Graziani , T. Gu , Y. Guan , K. Gudkova , C. Hadjivasiliou , H. Hayashii , S. Hazra , M. T. Hedges , W.-S. Hou , K. Inami , N. Ipsita , A. Ishikawa , R. Itoh , M. Iwasaki , W. W. Jacobs , Y. Jin , D. Kalita , C. H. Kim , D. Y. Kim , K.-H. Kim , Y.-K. Kim , K. Kinoshita , P. Kodyš , A. Korobov , S. Korpar , E. Kovalenko , P. Križan , P. Krokovny , T. Kuhr , R. Kumar , T. Kumita , A. Kuzmin , Y.-J. Kwon , Y.-T. Lai , T. Lam , J. S. Lange , L. K. Li , Y. Li , Y. B. Li , L. Li Gioi , J. Libby , D. Liventsev , T. Luo , Y. Ma , M. Masuda , T. Matsuda , S. K. Maurya , F. Meier , M. Merola , I. Nakamura , M. Nakao , Z. Natkaniec , L. Nayak , M. Nayak , S. Nishida , S. Ogawa , H. Ono , P. Pakhlov , G. Pakhlova , S. Pardi , H. Park , J. Park , S.-H. Park , A. Passeri , S. Patra , T. K. Pedlar , R. Pestotnik , L. E. Piilonen , T. Podobnik , E. Prencipe , M. T. Prim , G. Russo , S. Sandilya , L. Santelj , G. Schnell , C. Schwanda , Y. Seino , K. Senyo , W. Shan , C. Sharma , J.-G. Shiu , E. Solovieva , M. Starič , M. Sumihama , M. Takizawa , U. Tamponi , K. Tanida , F. Tenchini , R. Tiwary , K. Trabelsi , M. Uchida , Y. Unno , S. Uno , K. E. Varvell , E. Wang , S. Watanuki , E. Won , X. Xu , B. D. Yabsley , W. Yan , J. H. Yin , C. Z. Yuan , L. Yuan , Y. Yusa , Z. P. Zhang , V. Zhilich , and V. Zhukova 

(The Belle Collaboration)

We report the results of the first search for Standard Model and baryon-number-violating two-body decays of the neutral B mesons to Λ^0 and $\Omega_c^{(*)0}$ using 711 fb^{-1} of data collected at the $\Upsilon(4S)$ resonance with the Belle detector at the KEKB asymmetric-energy e^+e^- collider. We observe no evidence of signal from any such decays and set 95% confidence-level upper limits on the products of B^0 and \bar{B}^0 branching fractions for these two-body decays with $\mathcal{B}(\Omega_c^0 \rightarrow \pi^+\Omega^-)$ in the range between 9.5×10^{-8} and 31.2×10^{-8} .

PACS numbers: 11.30.Fs, 13.30.-a, 13.20.He

In the analysis presented in this Letter we search for new two-body B decays to final states with Λ^0 and Ω_c^0 , where Beyond the Standard Model (BSM) amplitudes could contribute directly or as the result of a Standard Model (SM) decay followed by baryon-antibaryon oscillations of Ω_c^0 or Λ^0 . Our analysis includes the SM Cabibbo-suppressed decay $\bar{B}^0 \rightarrow \bar{\Lambda}^0\Omega_c^{(*)0}$ and the BSM decay $\bar{B}^0 \rightarrow \bar{\Lambda}^0\bar{\Omega}_c^{(*)0}$. The former SM decay proceeds via the $b \rightarrow c$ tree transition and is poorly understood from a theoretical perspective because of hadronic uncertainties. The latter BSM decay could result from the $\Omega_c^0 - \bar{\Omega}_c^0$ oscillations, a scenario which was suggested recently [1] as a low-energy mechanism for baryon number violation (BNV), which is one of the three Sakharov's conditions for baryogenesis [2]. Additional BSM decays explored in our analysis include $\bar{B}^0 \rightarrow \Lambda^0\Omega_c^{(*)0}$, which is exceedingly unlikely in part due to the stringent limit recently set on $\Lambda^0 - \bar{\Lambda}^0$ oscillations by the BES III experiment [3]. A Feynman diagram for a quark-level SM

transition investigated in our analysis and a depiction of the $\Omega_c^0 - \bar{\Omega}_c^0$ BSM oscillation hypothesis are shown in Fig. 1.

To carry out the analysis described in this Letter we use the full Belle data sample of 711 fb^{-1} collected at the $\Upsilon(4S)$ resonance. This data sample contains 772 million $B\bar{B}$ pairs [4]. We search for two-body decays of the neutral B mesons to Λ^0 and one of the two Ω_c^0 states, Ω_c^0 or $\Omega_c(2770)^0$, previously known as Ω_c^{*0} (or their antiparticles). When we refer to either of these two Ω_c^0 states, we use the notation $\Omega_c^{(*)0}$. We reconstruct Ω_c^0 in its decay to π^+ and Ω^- , where Ω^- is detected in the $\Lambda^0 K^-$ channel. The Λ^0 is reconstructed via π^- and proton. The decay of B meson to Λ^0 and $\Omega_c(2770)^0$ is partially reconstructed: the radiative photon from the decay $\Omega_c(2770)^0 \rightarrow \gamma\Omega_c^0$, which is assumed to be the only decay of $\Omega_c(2770)^0$, is not explicitly reconstructed in the analysis.

Two final states, $\bar{\Lambda}^0\Omega_c^0$ and $\bar{\Lambda}^0\bar{\Omega}_c^0$, are studied in our analysis [5] of the decays of the neutral B mesons. The

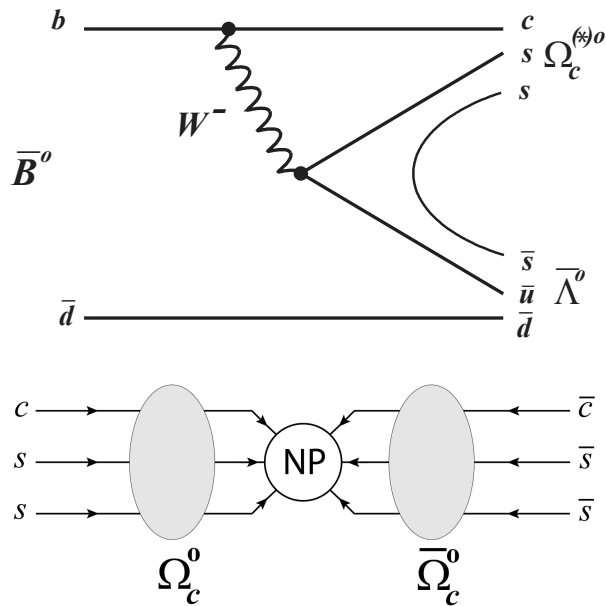


FIG. 1: Quark-level Feynman diagram for signal SM decays and a depiction of the $\Omega_c^0 - \bar{\Omega}_c^0$ oscillation hypothesis.

observation of the signal in the former final state would indicate the SM \bar{B}^0 decay, while the latter final state could be either due to the former SM decay followed by the $\Omega_c^0 - \bar{\Omega}_c^0$ oscillations or due to the direct BNV \bar{B}^0 decay. In this Letter, the final states $\bar{\Lambda}^0\Omega_c^0$ and $\bar{\Lambda}^0\bar{\Omega}_c^0$ are referred to as SM-compatible and exclusively-BSM channels, respectively. As we perform no B flavor tagging, any of the final states in this analysis could be attributed to \bar{B}^0 or B^0 ; therefore, when discussing the signal processes, we use the notation B to refer to either B^0 or \bar{B}^0 mesons. We report the results for the products of $\mathcal{B}(B \rightarrow \bar{\Lambda}^0\Omega_c^0)$, $\mathcal{B}(B \rightarrow \bar{\Lambda}^0\bar{\Omega}_c^0)$, $\mathcal{B}(B \rightarrow \bar{\Lambda}^0\Omega_c(2770)^0)$ and $\mathcal{B}(B \rightarrow \bar{\Lambda}^0\bar{\Omega}_c(2770)^0)$ with $\mathcal{B}(\Omega_c^0 \rightarrow \pi^+\Omega^-)$, where the latter branching fraction, quite interesting in its own right, has not been measured yet.

The Belle detector [6] is a large-solid-angle magnetic spectrometer that operated at the KEKB asymmetric-energy e^+e^- collider [7]. The detector components relevant to our study include a silicon vertex detector (SVD), a central drift chamber (CDC), a particle identification (PID) system that consists of a barrel-like arrangement of time-of-flight scintillation counters (TOF) and an array of aerogel threshold Cherenkov counters (ACC), and a CsI(Tl) crystal-based electromagnetic calorimeter (ECL). All these components are located inside a superconducting solenoid coil that provides a 1.5 T magnetic field.

To maximize discovery potential of the analysis and to validate the signal extraction procedure we use a sample of simulated background events referred to as generic

Monte Carlo (MC), equivalent to six times the integrated luminosity of the full Belle data sample. These events simulate hadronic continuum, i.e., quark-pair production in e^+e^- annihilation, the decay of the $\Upsilon(4S)$ resonance into pairs of B mesons and the subsequent decays of the latter according to known branching fractions [8]. Hadronic continuum represents the main source of background in our analysis. To estimate the overall reconstruction efficiency, we use several high-statistics signal MC samples, where the non-signal B meson decays generically. We use the MC generator EVTGEN [9] to simulate the production and decay processes at and near the production point of $\Upsilon(4S)$, and the GEANT toolkit [10] to model detector response and to handle the decays of Ω^- and Λ^0 . To model final state radiation, MC generator PHOTOS [11] is employed. Hadronization is modeled using MC generator PYTHIA [12].

In this analysis we exclusively reconstruct $\bar{\Lambda}^0\Omega_c^0$ ($\bar{\Lambda}^0\bar{\Omega}_c^0$) final state using six charged particles: three pions, a kaon, and a proton and an antiproton (two antiprotons). The selection criteria are optimized to suppress background in the SM-compatible channel and to reduce systematic uncertainties. Reconstructed charged particles are required to have p_\perp , the magnitude of the transverse part of their momenta with respect to the z axis which is opposite to the direction of the e^+ beam, larger than 50 MeV/ c . This requirement removes candidates found in the region where the efficiency has a large uncertainty and is very small. The efficiency of this selection for signal MC events is 28%, which is due to the kinematics of the signal process. To select signal particle candidates of the correct species, we apply requirements to the likelihood ratios, $R_{s/r} = L_s / (L_s + L_r)$, which are based on PID measurements [13], where L_s and L_r are the likelihoods according to the s and r particle species hypotheses, respectively. The likelihood for each particle species is obtained by combining information from CDC, TOF, ACC, and, for the electron/hadron likelihood ratio $R_{e/h}$, also ECL. Our requirements are $R_{\pi/K} \geq 0.6$ and $R_{e/h} \leq 0.95$ for pion from Ω_c^0 decay, $R_{K/\pi} \geq 0.4$ and $R_{e/h} \leq 0.95$ for kaon from Ω^- decay, and $R_{p/K} \geq 0.1$ for protons. The efficiency of PID requirements depends on the particle species and kinematics, and varies between 92% and 98%. PID misidentification rate is between 4% and 6% per particle. PID-based selection applied to all six charged particles used to reconstruct analyzed final states rejects 85% of background and is 71%-efficient for signal MC events.

Thus selected final state particles are used to reconstruct the following decays of signal baryon candidates: $\Lambda^0 \rightarrow p\pi^-$, $\Omega^- \rightarrow K^-\Lambda^0$, and $\Omega_c^0 \rightarrow \pi^+\Omega^-$. To identify the Λ^0 candidates, we search for secondary vertices associated with pairs of oppositely charged particles. To improve mass resolution and to suppress the combinatorial background, the tracks reconstructed for these particles are refit to a common vertex. The four-momenta

obtained from this kinematic fit are used for further analysis. The reconstructed mass of the Λ^0 candidate is required to be within $8 \text{ MeV}/c^2$ (5.4σ of Gaussian resolution) of the Λ^0 nominal mass [8]. To reconstruct an Ω^- candidate, we add together the four-momenta of Λ^0 and K^- candidates after refitting the Λ^0 vertex while constraining its reconstructed mass to the Λ^0 nominal mass. The reconstructed mass of the Ω^- candidate is required to be within $60 \text{ MeV}/c^2$ (15.1σ) of the Ω^- nominal mass [8]. Then the Ω^- candidate undergoes a procedure similar to the one used for Λ^0 candidates: we perform a vertex fit, update kinematics of the daughter particles, and require the reconstructed mass of the Ω^- candidate to be within $7 \text{ MeV}/c^2$ (4.4σ) of the Ω^- nominal mass [8], then we repeat a vertex fit with mass constraint. To suppress the combinatorial background, the distance between the interaction point and the decay vertex of Ω^- , i.e., decay length is required to be greater than 0.5 cm (6.5σ). This selection reduces background by 43% and, using SM signal channel with Ω_c^0 as a reference, keeps 83% of the signal. The procedure for reconstructing Ω_c^0 candidates is similar to the one used to reconstruct Ω^- when one replaces Λ^0 by Ω^- and K^- by π^+ , as well as requiring the invariant mass to be within $100 \text{ MeV}/c^2$ (17.5σ) before the vertex fit and $19 \text{ MeV}/c^2$ (4.1σ) after the vertex fit. The per-degree-of-freedom χ^2 from each kinematic fit in the described procedure is required to be less than 100. The overall efficiency of the vertex-mass χ^2 -based requirements is 83%, while the background is suppressed by a factor of approximately 10. The requirements applied to the reconstructed invariant masses after kinematic fitting are 91%-efficient and remove 89% of the remaining background.

To reconstruct signal B meson candidates, we use beam-energy-constrained B mass $M_{bc} \equiv \sqrt{E_{\text{beam}}^2/c^4 - p_B^2/c^2}$ and the energy difference $\Delta E \equiv E_B - E_{\text{beam}}$, where p_B , E_B , and E_{beam} are the momentum and energy of the B candidate, and the beam energy, respectively, evaluated in the e^+e^- center-of-mass frame. The momentum and energy of the B candidate are evaluated by adding together the four-momenta of Λ^0 and Ω_c^0 candidates after vertex fits with mass constraints. No vertex fit is performed for the B candidate, as doing so is found to have no tangible benefit for background suppression and separation between the Ω_c^0 and $\Omega_c(2770)^0$ signals. We require $M_{bc} > 5.200 \text{ GeV}/c^2$ and $-400 \text{ MeV} \leq \Delta E \leq 300 \text{ MeV}$. The efficiency of these last two selection criteria exceeds 99%. We define signal regions for final states with Ω_c^0 to be $M_{bc} > 5.270 \text{ GeV}/c^2$ and $-70 \text{ MeV} \leq \Delta E \leq 70 \text{ MeV}$, and for final states with $\Omega_c(2770)^0$ (where we ignore the radiative photon from the decay $\Omega_c(2770)^0 \rightarrow \gamma\Omega_c^0$) to be $M_{bc} > 5.265 \text{ GeV}/c^2$ and $-145 \text{ MeV} \leq \Delta E \leq -20 \text{ MeV}$. Each of the two

signal regions contains at least 98% of the respective signal. A slightly larger region, $M_{bc} > 5.260 \text{ GeV}/c^2$ and $-200 \text{ MeV} \leq \Delta E \leq 100 \text{ MeV}$, which includes the union of the two signal regions, is blinded. The non-blinded region of M_{bc} and ΔE defines the sideband. The defined regions are illustrated in Fig. 2.

When events contain more than one candidate (which occurs 4.2% of the time in signal MC, corresponding to the average candidate multiplicity of 1.05), we select the best candidate according to the smallest value of cumulative χ^2 obtained from the four vertex fits with mass constraints. Multiple candidates in this analysis are usually associated with particles of relatively low p_\perp , when multiple tracks with similar parameters are reconstructed for the same charged particle. We study signal MC events to prove that our procedure selects candidates with the best invariant mass and ΔE resolutions. Simulation demonstrates that, for events with multiple candidates, the best candidate selected by our method has all 6 signal particles reconstructed correctly in 93% of signal MC events. The best candidate is selected after applying all other analysis requirements. While the data and generic MC clearly contain Λ^0 and Ω_c^0 mesons, the distributions of M_{bc} and ΔE for simulation exhibit only non-peaking background, which is of combinatorial origin.

The background suppression and analysis sensitivity optimization are performed using the signal region for SM-compatible channel with Ω_c^0 . To suppress combinatorial background, the Ω^- decay length requirement is optimized by maximizing S/\sqrt{B} figure of merit (FOM), where S and B are the numbers of signal and background MC events satisfying this requirement. To provide better sensitivity to the SM signal, the requirements applied to the reconstructed invariant masses of Λ^0 , Ω^- and Ω_c^0 after the vertex fits are optimized by maximizing the value of Punzi's FOM [14]: $\varepsilon(t)/(a/2 + \sqrt{B(t)})$, where $\varepsilon(t)$ and $B(t)$ are the signal reconstruction efficiency and the number of background events expected in the signal region for a given set of requirements, t (applied to the reconstructed invariant masses), respectively. The quantity a is the desired significance in units of standard deviation. To predict $B(t)$, we multiply the number of events in the data sideband by the ratio of the numbers of events in the signal region and sideband in our generic MC sample. We require the optimized values of these selection criteria to be at least 4 units of Gaussian resolution away from the nominal masses [8]. This leads us to use $a = 10$. The choices made for the rest of the selection criteria represent a balance between maximizing the efficiency and minimizing the systematic uncertainties. The overall detection efficiencies for individual channels are in the range between 11.5% and 12.4%.

After applying all selection criteria, the total numbers of events remaining in data outside the blinded regions for final states $\bar{\Lambda}^0\Omega_c^0$ and $\bar{\Lambda}^0\bar{\Omega}_c^0$ are 16 and 2 events, respectively. Using MC simulation, we estimate that both

hadronic continuum and non-signal $B\bar{B}$ events contribute to the sideband. Using sideband data and the scaling factor of 0.10 ± 0.04 (0.09 ± 0.06) obtained from generic MC, we expect to find 1.6 ± 0.7 (0.18 ± 0.17) background events in the blinded region for SM-compatible (exclusively-BSM) channels.

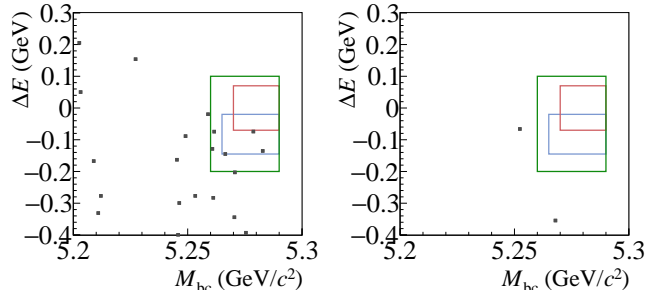


FIG. 2: The distributions of the best candidates in data events after applying all selection criteria in the analyzed region of ΔE vs M_{bc} for SM-compatible $\bar{\Lambda}^0\Omega_c^0$ (left) and exclusively-BSM $\bar{\Lambda}^0\Omega_c^0$ (right) reconstructed final states. The candidates are shown with square markers. The smaller boxes with red and blue outlines show the signal regions for final states with Ω_c^0 and $\Omega_c(2770)^0$, respectively. The larger box with a green outline represents the separation between the blinded region and the sideband.

Upon unblinding, in addition to the 16 events in the sideband, we find 5 events in the blinded region for the SM-compatible channels (of which 0 events are in the $\bar{\Lambda}^0\Omega_c^0$ signal region and 3 events are in the $\bar{\Lambda}^0\Omega_c(2770)^0$ signal region). In the exclusively-BSM channels, 2 events are observed, both outside the blinded region. The numbers of events observed in data are shown in Table I. The 2D distributions of ΔE vs M_{bc} for the best candidates in data events are shown in Fig. 2. The observation of 5 events in the SM blinded region including 3 events in the $\bar{\Lambda}^0\Omega_c(2770)^0$ signal region is consistent with SM background expectations. Statistical significance of such background fluctuation is less than 3 standard deviations. When we estimate the upper limits we assume that no background is expected in the signal region.

Numbers of events	Total	Blinded region	$\bar{\Lambda}^0\Omega_c^0$ signal region	$\bar{\Lambda}^0\Omega_c(2770)^0$ signal region
$\bar{\Lambda}^0\Omega_c^0$ data	21	5	0	3
Background	N/A	1.6 ± 0.7	0.44 ± 0.45	0.44 ± 0.45
$\bar{\Lambda}^0\Omega_c^0$ data	2	0	0	0
Background	N/A	0.18 ± 0.17	0.00 ± 0.12	0.12 ± 0.15

TABLE I: Numbers of events observed in data and background estimates.

Systematic uncertainties arise from imprecise knowledge of various efficiencies and other quantities detailed in Table II. We assign a 0.35% uncertainty for tracks reconstructed for charged particles with $p_\perp > 200$ MeV/c [15] and a 1.2% uncertainty for particles with 50 MeV/c $\leq p_\perp \leq 200$ MeV/c [16]. Therefore, based on the fractions of signal MC particles in these two momentum regions, we assign 2.9% to total uncertainty for all six tracks. Uncertainties due to PID selection for charged kaons and pions are obtained from high-statistics comparisons between MC and data [17]. As no dedicated study has been performed for the 98%-efficient proton PID requirement $R_{p/K} \geq 0.1$, we assign a 2% uncertainty on basis of its high efficiency. To estimate the magnitudes of possible MC-data differences in the efficiencies of selection criteria applied to the Ω^- decay length, χ^2 from kinematic fits and the reconstructed masses, we vary selection criteria within ranges typical for Belle analyses as described below. Uncertainties for the requirements applied to the Ω^- decay length and reconstructed masses are determined by varying the values of selection criteria by $\pm 10\%$ and using the change in the efficiency as an estimate of systematic uncertainty. Similarly, the systematic uncertainty in the efficiency of the vertex-mass kinematic fits χ^2 criteria is estimated as the larger change in reconstruction efficiency for signal MC when the χ^2 requirement is varied by ± 25 with respect to the nominal value of 100. Total uncertainty for M_{bc} and ΔE selection criteria is estimated to be 0.5% which is half of their inefficiency. Uncertainties on daughter branching fractions, $\mathcal{B}(\Omega^- \rightarrow \Lambda^0 K^-) = 0.678$ and $\mathcal{B}(\Lambda^0 \rightarrow p\pi^-) = 0.641$, and on the number of $B^0\bar{B}^0$ pairs in Belle data, $N_{B^0\bar{B}^0} = 374 \times 10^6$, are taken from References [8] and [4, 18], respectively. Relative difference between efficiencies for the charge conjugate final states in MC is approximately 0.4%. This detector charge asymmetry arises because of the difference in the detector response to particles and antiparticles. While simulation is known to underestimate this effect, in our analysis its impact is reduced because we combine charge conjugate final states in efficiency estimates. To account for limitations of our approach, a relative systematic uncertainty of 0.8% is assigned to the efficiencies, which is twice of the MC-predicted difference between efficiencies of individual charge conjugate states. Possible presence of BSM amplitudes could affect angular distributions of baryons in the signal decay chain. This effect is likely to be small in decays of pseudoscalar B meson. To be conservative, we assign relative systematic uncertainty of 0.5% based on MC studies of efficiency's dependence on helicity angles, i.e., baryons' polarization. Finally, relative uncertainty due to MC statistics is determined using the formula $\sqrt{\epsilon \times (1 - \epsilon)/N} \times (1/\epsilon)$, where ϵ is the overall signal reconstruction efficiency and N is the number

of signal MC events (before reconstruction). We combine the uncertainties for all contributions in quadrature, while taking into account also the 100% correlation between two $\Lambda^0 \rightarrow p\pi^-$ decays, two protons and correlated selection criteria for reconstructed masses, to estimate overall systematic uncertainty σ_r to be 6.2%.

Source	Uncertainty (%)
Track reconstruction (overall)	2.9
π^+ PID (for $\Omega_c^0 \rightarrow \pi^+\Omega^-$)	0.8
K^- PID (for $\Omega^- \rightarrow K^-\Lambda^0$)	1.4
p PID (for Λ^0 decays)	2×1.0
Decay length (Ω^-)	2.0
Reconstructed masses	4×0.5
Vertex fits (χ^2)	1.5
M_{bc} and ΔE	0.5
$\mathcal{B}(\Omega^- \rightarrow \Lambda^0 K^-)$	1.0
$\mathcal{B}(\Lambda^0 \rightarrow p\pi^-)$	2×0.7
$N_{B^0\bar{B}^0}$	2.9
Detector charge asymmetry	0.8
Polarization of baryons	0.5
MC statistics	0.7
Overall (σ_r)	6.2

TABLE II: Summary of relative systematic uncertainties.

We estimate the 95% CL upper limits on the products of branching fractions $\mathcal{B}(B \rightarrow \bar{\Lambda}^0\Omega_c^{(*)0}) \times \mathcal{B}(\Omega_c^0 \rightarrow \Omega^-\pi^+)$ as $U_n/(2 \times N_{B^0\bar{B}^0} \times \epsilon \times \mathcal{B}(\Omega^- \rightarrow \Lambda^0 K^-) \times \mathcal{B}(\Lambda^0 \rightarrow p\pi^-)^2)$, where B is assumed to be solely either B^0 or \bar{B}^0 , and U_n is the 95% CL upper limit on the number of events. Systematic uncertainties are included using the approach by Cousins and Highland [19]: $U_n = U_{n0}(1 + (U_{n0} - n)\sigma_r^2/2)$, where n is the number of events observed in data in the signal region (including charge-conjugate final state). To estimate U_{n0} , the 95% CL upper limit on the number of events in data without systematic uncertainties, we use the upper bounds of the 90% CL intervals tabulated in the seminal paper by Feldman and Cousins [20]. When using these confidence intervals, we assume that no background events are expected in either signal region. For the channel where 3 events are observed, we extend the lower bound of the respective CL interval to 0. This procedure is motivated by a large uncertainty in background estimates and results in overcoverage. Various quantities necessary to complete the calculations are shown in Tables II and III. Following the procedure described above, we summarize the resulting 95% CL upper limits in Table IV. The upper limits on the products of branching

fractions $\mathcal{B}(B \rightarrow \bar{\Lambda}^0\bar{\Omega}_c^{(*)0}) \times \mathcal{B}(\Omega_c^0 \rightarrow \Omega^-\pi^+)$ are estimated similarly.

Channel	$\bar{\Lambda}^0\Omega_c^0$	$\bar{\Lambda}^0\Omega_c(2770)^0$	$\bar{\Lambda}^0\bar{\Omega}_c^0$	$\bar{\Lambda}^0\bar{\Omega}_c(2770)^0$
ϵ (%)	12.1	11.5	12.4	11.8
n (events)	0	3	0	0
U_{n0} (events)	2.44	7.42	2.44	2.44
U_n (events)	2.45	7.48	2.45	2.45

TABLE III: Information needed for upper limit estimates.

In summary, we use the full data sample recorded by the Belle experiment at the $\Upsilon(4S)$ resonance to search for SM and BNV two-body decays of neutral B mesons to Ω_c^0 or $\Omega_c(2770)^0$, and Λ^0 . We observe no statistically significant signals and set 95% CL upper limits in the range between 9.5×10^{-8} and 31.2×10^{-8} on the products of neutral B meson branching fractions to Λ^0 and $\Omega_c^{(*)0}$ with $\mathcal{B}(\Omega_c^0 \rightarrow \pi^+\Omega^-)$. The analysis presented in this Letter is the first study of such SM-compatible and exclusively-BSM decays.

This work, based on data collected using the Belle detector, which was operated until June 2010, was supported by the Ministry of Education, Culture, Sports, Science, and Technology (MEXT) of Japan, the Japan Society for the Promotion of Science (JSPS), and the Tau-Lepton Physics Research Center of Nagoya University; the Australian Research Council including grants DP210101900, DP210102831, DE220100462, LE210100098, LE230100085; Austrian Federal Ministry of Education, Science and Research (FWF) and FWF Austrian Science Fund No. P 31361-N36; National Key R&D Program of China under Contract No. 2022YFA1601903, National Natural Science Foundation of China and research grants No. 11575017, No. 11761141009, No. 11705209, No. 11975076, No. 12135005, No. 12150004, No. 12161141008, and

Quantity ($\times \mathcal{B}(\Omega_c^0 \rightarrow \Omega^-\pi^+)$)	Upper limit (at 95% CL)
$\mathcal{B}(B \rightarrow \bar{\Lambda}^0\Omega_c^0)$	9.7×10^{-8}
$\mathcal{B}(B \rightarrow \bar{\Lambda}^0\Omega_c(2770)^0)$	31.2×10^{-8}
$\mathcal{B}(B \rightarrow \bar{\Lambda}^0\bar{\Omega}_c^0)$	9.5×10^{-8}
$\mathcal{B}(B \rightarrow \bar{\Lambda}^0\bar{\Omega}_c(2770)^0)$	10.0×10^{-8}

TABLE IV: Summary of the results.

No. 12175041, and Shandong Provincial Natural Science Foundation Project ZR2022JQ02; the Czech Science Foundation Grant No. 22-18469S; Horizon 2020 ERC Advanced Grant No. 884719 and ERC Starting Grant No. 947006 “InterLeptons” (European Union); the Carl Zeiss Foundation, the Deutsche Forschungsgemeinschaft, the Excellence Cluster Universe, and the VolkswagenStiftung; the Department of Atomic Energy (Project Identification No. RTI 4002), the Department of Science and Technology of India, and the UPES (India) SEED finding programs Nos. UPES/R&D-SEED-INFRA/17052023/01 and UPES/R&D-SOE/20062022/06; the Istituto Nazionale di Fisica Nucleare of Italy; National Research Foundation (NRF) of Korea Grant Nos. 2016R1-D1A1B02012900, 2018R1A2B3003643, 2018R1A6A1A-06024970, RS202200197659, 2019R1I1A3A01058933, 2021R1A6A1A03043957, 2021R1F1A1060423, 2021R1-F1A1064008, 2022R1A2C1003993; Radiation Science Research Institute, Foreign Large-size Research Facility Application Supporting project, the Global Science Experimental Data Hub Center of the Korea Institute of Science and Technology Information and KREONET/GLORIAD; the Polish Ministry of Science and Higher Education and the National Science Center; the Ministry of Science and Higher Education of the Russian Federation and the HSE University Basic Research Program, Moscow; University of Tabuk research grants S-1440-0321, S-0256-1438, and S-0280-1439 (Saudi Arabia); the Slovenian Research Agency Grant Nos. J1-9124 and P1-0135; Ikerbasque, Basque Foundation for Science, and the State Agency for Research of the Spanish Ministry of Science and Innovation through Grant No. PID2022-136510NB-C33 (Spain); the Swiss National Science Foundation; the Ministry of Education and the National Science and Technology Council of Taiwan; and the United States Department of Energy and the National Science Foundation. These acknowledgements are not to be interpreted as an endorsement of any statement made by any of our institutes, funding agencies, governments, or their representatives. We thank the KEKB group for the excellent operation of the accelerator; the KEK cryogenics group for the efficient operation of the solenoid; and the KEK computer group and the Pacific Northwest National Laboratory (PNNL) Environmental Molecular Sciences Laboratory (EMSL) computing group for strong computing support; and the National Institute of Informatics, and Science Information NETwork 6 (SINET6) for valuable network support.

- Baryons. *Phys. Rev. D*, 96(7):075009 (2017).
- [2] A.D. Sakharov, Violation of CP Invariance, C Asymmetry, and Baryon Asymmetry of the Universe. *Sov. Phys. Usp.*, 34(5):392 (1991).
- [3] M. Ablikim *et al.* (BES III Collaboration), Search for $\bar{\Lambda} - \Lambda$ baryon-number-violating oscillations in the decay $J/\psi \rightarrow pK^- \Lambda + c.c.$, *Phys. Rev. Lett.* **131**, 121801 (2023).
- [4] J. Brodzicka *et al.*, Physics Achievements from the Belle Experiment. *Prog. Theor. Exp. Phys.*, 04D001 (2012).
- [5] The inclusion of charge-conjugate decay modes is implied throughout this Letter, unless stated otherwise.
- [6] A. Abashian *et al.* (Belle Collaboration), The Belle Detector. *Nucl. Instrum. Meth. A*, 479:117 (2002); also see Section 2 in Ref. [4].
- [7] S. Kurokawa and E. Kikutani, Overview of the KEKB Accelerators. *Nucl. Instrum. Meth. A*, 499:1 (2003), and other papers included in this Volume; T. Abe *et al.*, Achievements of KEKB. *Prog. Theor. Exp. Phys.*, 03A001 (2013) and references therein.
- [8] R. L. Workman *et al.* (Particle Data Group), Review of Particle Physics. *Prog. Theor. Exp. Phys.*, 083C01 (2022) and 2023 update.
- [9] D.J. Lange, The EvtGen Particle Decay Simulation Package. *Nucl. Instrum. Meth. A*, 462:152 (2001).
- [10] R. Brun *et al.*, GEANT Detector Description and Simulation Tool, CERN *ebook*, 10.17181/CERN.MUHF.DMJ1 (1994).
- [11] E. Barberio, B. van Eijk and Z. Was, PHOTOS: A Universal Monte Carlo for QED radiative corrections in decays. *Comput. Phys. Commun.*, 66:115 (1991).
- [12] T. Sjostrand, S. Mrenna and P. Z. Skands, A Brief Introduction to PYTHIA 8.1, *Comput. Phys. Commun.* **178**, 852 (2008).
- [13] See Ch. 5 in A. J. Bevan, B. Golob, Th. Mannel, S. Prell, and B. D. Yabsley (eds), The Physics of the B Factories, *Eur. Phys. J. C*, 74:3026 (2014); SLAC-PUB-15968; KEK Preprint 2014-3.
- [14] G. Punzi, Sensitivity of Searches for New Signals and Its Optimization. *eConf C*, 030908:MODT002 (2003).
- [15] S. Ryu *et al.* (Belle Collaboration), Measurements of Branching Fractions of τ Lepton Decays with One or More K_S^0 . *Phys. Rev. D*, 89(7):072009 (2014).
- [16] P. Chen *et al.* (Belle Collaboration), Observation of $B^- \rightarrow \bar{p}\Lambda D^0$ at Belle. *Phys. Rev. D*, 84:071501 (2011).
- [17] E. Nakano, Belle PID. *Nucl. Instrum. Meth. A*, 494:402 (2002)
- [18] S. Choudhury *et al.* (Belle Collaboration), Measurement of the B^+/B^0 production ratio in e^+e^- collisions at the $\Upsilon(4S)$ resonance using $B \rightarrow J/\psi(l)K$ decays at Belle. *Phys. Rev. D* **107**, no.3, L031102 (2023).
- [19] R. Cousins and V. Highland, Incorporating Systematic Uncertainties Into an Upper Limit. *Nucl. Instrum. Meth. A*, 320:331 (1992).
- [20] G. J. Feldman and R. D. Cousins, A Unified Approach to the Classical Statistical Analysis of Small Signals. *Phys. Rev. D*, 57:3873 (1998).

[1] K. Aitken, D. McKeen, T. Neder, and A.E. Nelson, Baryogenesis from Oscillations of Charmed or Beautiful